Towards Timely Alzheimer Diagnosis: a Self-Powered Amperometric Biosensor for the Neurotransmitter Acethylcholine

Felismina T.C. Moreira[b], Goreti F. Sale[b], Mirella Di Lorenzo[a].*

[a] University of Bath, Department of Chemical Engineering, Bath, BA2 7AY, UK

[b]BioMark-CINTESIS/ISEP, School of Engineering, Polytechnic Institute of Porto, Portugal

*Corresponding author:

Email: M.Di.Lorenzo@bath.ac.uk

Telephone: +44(0)1225 385574

Abstract

Serious brain disorders, such as the Alzheimer's Disease (AD), are associated with a marked drop in the levels of important neurotransmitters, such as acetylcholine (ACh). Real time monitoring of such biomarkers can therefore play a critical role in enhancing AD therapies by allowing timely diagnosis, verifications of treatment effectiveness, and developments of new medicines. In this study, we present the first acetylcholine/oxygen hybrid enzymatic fuel cell for the self-powered on site detection of ACh in plasma, which is based on the combination of an enzymatic anode with a Pt cathode. Firstly, an effective acetylcholinesterase immobilized electrode was developed and its electrochemical performance evaluated. Highly porous gold was used as the electrode material, and the enzyme was immobilized *via* a one step rapid and simple procedure that does not require the use of harsh chemicals or any electrode/enzyme pre-treatments. The resulting enzymatic electrode was subsequently used as the anode of a miniature flow-through membrane-less fuel cell and showed excellent response to varying concentrations of ACh. The peak power generated by the fuel cell was 4 nW at a voltage of 260 mV and with a current density of 9 μA cm^{-2}. The limit of detection of the fuel cell sensor was 10 μM, with an average response time as short as 3 minutes. These exciting results open new horizons for point-of-care Alzheimer diagnosis and provide an attractive potential alternative to established methods that require laborious and time-consuming sample treatments and expensive instruments.

Keywords:

Enzymatic Fuel Cell, Acetylcholinesterase, Acetylcholine, Highly Porous Gold, Alzheimer.

1. INTRODUCTION

~~Dementia describes a set of symptoms that include memory loss and difficulties with thinking, problem-solving and language.~~ Worldwide, over 35 million people are currently diagnosed with dementia. This number ~~that~~ is estimated to double every 20 years in aging populations, thus reaching a value of 65.7 million in 2030, and of 115.4 million in 2050 (Prince et al. 2015). The most common cause of senile dementia is the Alzheimer's disease (AD), with currently over 17 million cases worldwide (Mayeux and Schupf 2011). AD is characterized by the progressive loss of cognitive function and personality changes. Early detection of AD, as well as the capability to distinguish it from other forms of dementia, is key to plan timely caring actions and help families intervene before the disease becomes too serious. Yet, so far, there are no definitive diagnostic tests that allow accurate and effective early detection of this condition. The diagnosis of AD occurs typically *via* extensive clinical examinations based on specific clinical diagnostic criteria that have been established in 1984 by the National Institute of Neurological and Communicative Disorders and Stroke (NINCDS) and the Alzheimer's Disease and Related Disorders Association (ADRDA), known as the NINCDS-ADRDA Alzheimer's criteria (McKhann et al. 1984).

The identification of relevant biomolecules that could act as AD biomarkers, and therefore allow rapid and effective diagnosis of this disease, is of particular relevance. Recent studies have suggested that systemic signs caused by concentration changes of specific biomolecules, which include mostly the Amyloid-β and Tau proteins present in cerebrospinal fluid (CSF) and plasma, can be associated with the progression of AD (Kanai et al. 1998). A particularly promising route to diagnose AD is, however, represented by the possibility to monitor the levels of neurotransmitters, such as acetylcholine (ACh), in cerebrospinal fluid. ACh is one of the first identified neurotransmitters and is found in the peripheral and central nerve system of the brain (Cannon et al. 2004; Hou et al. 2012). The role of ACh is to transmit messages from motor

nerves to muscles, especially to the heart, bladder and stomach, and ACh is involved in several functions, including cognition, memory and movement (Hasselmo and Sarter 2010; Van der Zee and Luiten 1999). The dysfunction in ACh regulation in the brain causes neuropsychiatric disorders such as Alzheimer's disease, Parkinson's disease, progressive dementia, Myasthenia Gravis and schizophrenia (Davis and Berger 1979; Tandon 1999). Considering the importance of this biomolecule, there is high interest in developing methods for its *in vivo* quantification (Garris and A 2010). Real-time monitoring of extra-cellular concentration changes of ACh would in fact allow understanding the function of the nervous system and the association to AD, examining the degeneration of cholinergic neural systems in AD, and evaluating pharmaceuticals that affect cholinergic activity at the single cell level (Mitchell 2004; Nguyen et al. 2010). Nonetheless, current methods to determine ACh levels in body fluids, such as ELISA (Hinman et al. 1986; Kawanami et al. 1984) and microdialysis sampling combined to offline analysis by liquid chromatography with mass spectroscopy detection (Nirogi et al. 2010; Song et al. 2012; Uutela et al. 2005), are laborious, expensive, slow and not suitable for *in situ* monitoring.

Electrochemical sensors are capable of fast *in situ* detection sensors and, therefore, offer a powerful avenue for real time diagnostics that overcomes the drawback of traditional analytical methods (Wilson and Gifford 2005). In particular, the detection of ACh and its metabolite choline (Ch) has been successfully demonstrated with enzyme-based amperometric sensors. Depending on the specific target, the sensors use either acetylcholine esterase (AChE) or choline oxidase (ChOx), as well as both enzymes together (Garguilo and Michael 1995; Hou et al. 2012; Mitchell 2004; Wise et al. 2002). ~~AChE-based sensors have been also suggested for the detection of toxic organophosphorous pesticides that, by inhibiting the activity of this enzyme, lead to toxic levels of acethylcholine in the cells, with severe threat to human health (Cai et al. 2014; Kaur and Srivastava 2015).~~

In this work, we propose the first hybrid enzymatic fuel cell (EFC)-based sensor for the real time and *in situ* detection of ACh. EFCs are a particular type of fuel cells that use enzymes to catalyse the direct generation of electricity from physiological fluids under body temperature and pressure (Barton et al. 2004) ~~(du Toit and Di Lorenzo 2015)~~. As such, EFC provide an attractive possibility for implantable and wearable diagnostic devices (Leech et al. 2012) ~~(du Toit et al. 2016).~~ Preliminary proof-of-concept studies in this direction are highly encouraging. EFCs have been successfully implanted in living organisms, thus showing electricity generation from physiological fluids, such as blood and plasma (Castorena-Gonzalez et al. 2013; Halámková et al. 2012; MacVittie et al. 2013). Some successful examples of wearable EFCs have also been reported, such as the tattoo EFC that generates electricity from lactate in sweat (Jia et al. 2013) and the contact lens that uses the glucose in tears as fuel (Reid et al. 2015). Considering that within a specific range the power generated is proportional to the amount of substrate (the analyte) in the input solution, the most intuitive use of EFCs is as self-powered amperometric sensors for that substrate. By varying the nature of the enzyme(s) employed, several biomarkers of interest could be detected. The majority of the EFCs reported so far, uses the enzymes glucose oxidase and glucose dehydrogenase and focus on the detection of glucose (Ivanov et al. 2010). An EFC embedded into microfluidic follow-channels paper was reported for the detection of the carcinoembryonic antigen (Li et al. 2015). Successful examples of EFC applications as sensor for the detection of lactate (Katz et al. 2001), cyanide (Deng et al. 2010), mercury ion (Wen et al. 2011) and cholesterol (Sekretaryova et al. 2014) have also been reported.

The innovative ~~enzymatic~~ fuel cell reported in the present work utilizes at the anode the enzyme acetylcholinesterase (AChE), which is immobilized onto a nanostructured electrode made of a highly porous gold (hPG) coated onto a Pt surface. The use of nanostructured electrode materials is key to improve the enzyme loading and enhance the electrochemical

performance of EFCs (Ivanov et al. 2010). hPG in particular has proven to be an excellent candidate for EFCs, given its large specific surface area, biocompatibility and non-toxicity (du Toit and Di Lorenzo 2014b). In this study, we used a rapid and simple one-step electrochemical process to immobilise AChE onto hPG that does not require complex or laborious electrode and/or enzyme pre-treatments. The first part of this study focus on investigating the electrochemical performance of the resulting electrode. Subsequently, the enzymatic electrode is tested as the anode of a flow-through membrane-less fuel cell and the current and power output is recorded for a series of ACh concentrations, thus proving its use as online sensor.

2. EXPERIMENTAL SECTION

2.1 Materials

All the chemicals were of analytical reagent grade and were used without further purification. Acetylcholinesterase from *Electrophorus electricus*, 500 U, was purchased from Sigma-Aldrich. The Saturated Calomel Electrode (SCE), used as the reference electrode, was purchased from IJCambria Ltd. Platinum wire (diameter: 0.5 mm) was purchased from Cookson Precious Metals Ltd. Polydimethylsiloxane (PDMS, Dow Corning Sylgard 184) was purchased from Ellsworth Adhesives.

All aqueous solutions used were prepared using reverse osmosis purified water. The phosphate buffered saline (PBS) solution was prepared on a weekly basis and consisted of 137 mM NaCl, 2.7 mM KCl, 10 mM Na_2HPO_4, 2 mM KH_2PO_4. The pH of the resulting solution was adjusted to a value of 7.4 with the drop-wise addition of HCl or NaOH. Glycine buffer was prepared by

mixing 0.01 M of Glycine with 0.1 M of NaCl and by adjusting the pH to 7.4 by drop-wise addition of NaOH and HCl.

All potentiostatically-controlled electrochemical processes were performed using the Autolab PGSTAT128 N (Metrohm, UK) potentiostat. The moulds for the PDMS structures were 3D printed in polylactic acid using a Makerbot Replicator.

2.2 Preparation of the electrodes

The electrodes were prepared by electrodepositing a film of highly porous gold (hPG) onto Pt wires *via* a hydrogen bubbling template, as previously described (du Toit and Di Lorenzo 2014a). Briefly, the platinum wires were immersed in an electrolyte consisting of 0.1 M $HAuCl_4$ and 1 M NH_4Cl and gold was deposited by gradually stepping down the working potential as follows: -0.7 V (vs. SCE) for 5 s; -1.5 V (vs. SCE) for 5 s; -2.5 V (vs. SCE) for 5 s and-4.0 V (vs. SCE) for 10 s. This process was performed in a three electrode set-up, with platinum as the counter electrode and SCE as the reference electrode. This set-up was also used for the immobilization of AChE onto the hPG/Pt electrode. The electrodes were immerged in a PBS buffer (pH 7.4) containing 6.25 U mL^{-1} of enzyme, and a potential of 0.6 V vs SCE was applied for one hour, according to the immobilization protocol previously established by our group (du Toit et al. 2016).

The electrochemical response of both AChE/hPG/Pt and hPG/Pt electrodes to ACh, within the range of 2- 2400 µg mL^{-1}, was evaluated by both chronoamperometry (CA) and Square Wave Voltammetry (SWV) in the conventional three-electrode set-up (SCE as the reference electrode, Pt as the counter electrode). During the test, ACh was drop-wise added to the buffer solution

until the target concentration. The solution was then stirred for 30 seconds before the measurement. The response to ACh was evaluated in terms of current variation, $\Delta i = i_c - i_0$, where, i_c is the observed current at the set concentration and i_0 is the baseline current in the absence of substrate.

The sensitivity towards ACh was obtained from the slope, b ($\mu A\ mM^{-1}$), of the calibration curve and was referred to the total surface area, A (cm^2), of the electrode as:

$$sensitivity = \frac{b}{A}$$

The electrodes performance was also tested by cyclic voltammetry at a scan rate of 50 mV s^{-1} in the presence and absence of ACh. The tests were performed both in the presence and absence of oxygen. In the latter case, nitrogen was purged in the electrolyte for 15 min before the test.

For the case of the enzymatic electrode, the affinity towards ACh was estimated in terms of the apparent Michaelis-Menten constant (K_m^{app}). This was calculated by using the electrochemical version of the Lineweaver-Burk equation of enzyme kinetics, as previously described (du Toit and Di Lorenzo 2014b):

$$\frac{1}{i} = \frac{1}{i_{max}} + \frac{K_M^{app}}{i_{max}\, c}$$

Where i is the steady-state current observed after the addition of glucose; i_{max} is the maximum current under the saturated concentration of glucose; c is the ACh concentration.

2.3 Fuel cell fabrication and operation

The single-chamber membrane-less hybrid EFC used in this work was fabricated in PDMS from a 3D printed mould, as previously described (du Toit et al. 2016). The device consisted of a

single chamber of 6 mm x 1 mm x 17 mm, hosting a AChE/hPG/Pt wire (the anode) and a Pt wire (as a combined counter/reference electrode), placed parallel to each other following the direction of flow. Each electrode was 10 mm long, with a total surface area exposed to the channel of 0.16 cm^2.

The inlet and outlet streams of the device were connected to a programmable multichannel peristaltic pump (Gilson, Miniplus 3), equipped with 2-stopped pump tubing. The device was continuously fed with an aerated PBS solution containing ACh (range: 2- 2400 μg mL^{-1}) at a rate of 0.4 ml min^{-1}. During the operation, the electrodes were connected to an external circuit with an external fixed resistance (R_{ext}) of 80 kΩ and to a PicoLog ADC-24 multichannel data logger to monitor the cell voltage (V). The current output (I) was calculated using Ohm's law (I=V/ R_{ext}) and the power was calculated as P= VI. Figure 1 shows the principle of operation of the AChE fuel cell.

Polarisation tests were performed by Linear Sweep Voltammetry (LSV) using a scan rate of 1.0 mV s^{-1}, from the open circuit potential (OCP) to lower voltage regions.

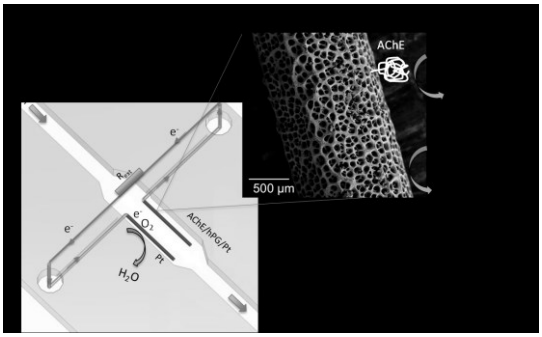

Figure 1. Design and working principle of the AChE fuel cell. The fuel cell consists of a membrane-less single channel that operates in flow-though mode. The cell hosts an anode (Pt wire coated with a film of highly porous gold, hPG) and a cathode, (Pt wire) connected to a external circuit with a fixed external load (R_{ext}). AChE is immobilised onto the anode surface and catalyses the first step of oxidation of ACh, while hPG catalyses the

second. The electrons generated flow through the external circuit, thus producing a current output that is correlated to the amount of ACh oxidized. The reaction is completed at the cathode where the electrons combine with the protons and the oxygen to generate water.

3. RESULTS AND DISCUSSION

3.1 Electrochemical characterization of the AChE/hPG/Pt electrode

The first part of this study concerned the development of an effective bioelectrode for ACh detection. To maximize the enzyme loading and facilitate direct electron transfer, highly porous gold structures were selected as the electrode material. Nanostructured electrode materials, such as hPG, have recently aroused tremendous interest, due to their large specific surface area leading to enhanced electron-transfer kinetics and their great biocompatibility (Kang and Lee 2016). The immobilization of AChE onto hPG was achieved by electrochemical adsorption, through the rapid, efficient and low-cost methodology previously established by our group (du Toit and Di Lorenzo 2014b). At the physiological pH of 7.4 used in this study AChE has a negative charge (isoelectric point between 5.6 and 6.0). A potential of 0.6 V (vs SCE) was therefore chosen for its electrostatic immobilization to allow the building-up of a net positive charge onto the hPG electrode surface that would attract the oppositely charged enzyme. The electrochemical performance of the resulting AChE/hPG/Pt electrode was tested by SWV and CV in a conventional three-electrode set up, with SCE as the reference electrode and platinum wire as the auxiliary electrode (Figure 2). The electrochemical response of AChE/hPG/Pt was investigated in the absence (a) and presence (b) of 17 mM of acetylcholine, and compared with the case of the non-enzymatic hPG/Pt electrode (c). Initially the electrodes were tested in PBS

buffer. As shown in Figure 2A and 2C, the AChE/hPG/Pt electrode responded to the addition of ACh in solution with an up-shift in the SWV and CV curves in correspondence to 0.3 V.

AChE hydrolyses ACh to choline and acetic acid, according to the following reaction (Step 1):

$$\mathrm{ACh} + \mathrm{H_2O} \xrightarrow{\mathrm{AChE}} \mathrm{CH_3COOH} + \mathrm{Ch}$$

Usually, the detection of ACh is achieved by the combined use of the enzyme AChE with choline oxidase, ChO, to allow the oxidation of Ch into H_2O_2, which is then electrochemically monitored (Kanik et al. 2013; Mitchell 2004). In the specific case of this study, the functional group(s) of Ch are instead directly electro-oxidised by hPG to generate oxidized intermediate(s), according to the following suggested reaction (Step 2):

$$\mathrm{Ch} + \mathrm{O_2} \xrightarrow{\mathrm{hPG}} \text{oxidised intermediate(s)} + \mathrm{H^+} + \mathrm{e^-}$$

The peak observed in both the SWV and CV curves is therefore related to Ch oxidation at the working electrode and is a consequence of AChE activity. The electro-oxidation of choline on nanostructured electrode structures has been already reported for the case of a nickel oxide nanostructured electrode (Sattarahmady et al. 2014). In particular, it was suggested that the process involves the oxidation of functional group(s) of Ch in either a single or multiple step. A similar process was suggested for thiocholine by Chauhan et al. with an iron nanoparticles/multiwalled carbon nanotubes modified gold electrode (Chauhan and Pundir 2011).

The hPG/Pt electrode also showed good reactivity towards ACh, with an oxidation peak at 0.27 V (vs. SCE) (Figure 2A), which might be related to the oxidation of phosphate (du Toit and Di Lorenzo 2014a). To investigate this further, and study the interference of phosphate in the

electrochemical measurements, these tests were repeated in glycine buffer (Figure 2B and 2C). In the case of the AChE/hPG/Pt electrode, the oxidation peak at 0.30 V was confirmed. The response to ACh was, however, approximately two times higher than in buffer, with a $\Delta I \approx 0.04$ mA. Moreover, the intensity of the peak produced by hPG/Pt in glycine, was of only 0.01 mA. This value is 20% lower than the case of PBS, thus confirming the interference of phosphate. The two peaks observed in the SWV curves, probably related to oxidation reactions occurring onto the hPG surface, might have been masked in the case of PBS by the much larger peak related to phosphate oxidation.

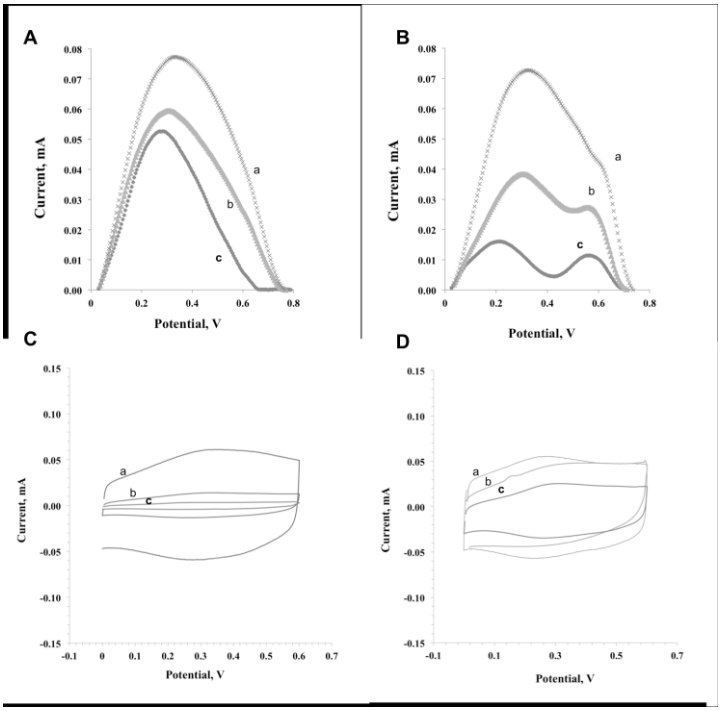

Figure 2 Electrochemical Square Wave Voltammetry (SWV) and Cyclic Voltammetry (CV) responses to ACh of the enzymatic and non-enzymatic hPG/Pt electrodes in PBS buffer (A, C) and glycine buffer (B, D). a) AChE/hPG/Pt electrode in the presence of 17 mM of ACh; b) AChE/hPG/Pt electrode in the absence of ACh; c) control, hPG/Pt electrode in buffer. The scan rate was of 50 mV s^{-1}.

The response of both the enzymatic and non-enzymatic electrode to increasing ACh concentrations was subsequently tested by SWV and CA (at 0.3 V vs SCE). The results are reported in Figure 3. Both electrodes showed a very good response to ACh, and generated an output current signal proportional to its concentration. Considering its high reactivity, the response of hPG/Pt to ACh was not surprising (du Toit and Di Lorenzo 2014a). Although the electrocatalytic oxidation of ACh on nanostructured electrodes has already been shown (Sattarahmady et al. 2013), this is the first time that it is proven also for the case of porous gold. The type of buffer used had an influence on the response. Generally, in glycine the current generated by AChE/hPG/Pt was higher than hPG/Pt (Figure 3B and 3E), since there was no interference with phosphate in the reading. On the other hand, hPG/Pt generated a higher (Figure 3C) or very similar (Figure 3F) current than the enzymatic electrode in PBS.

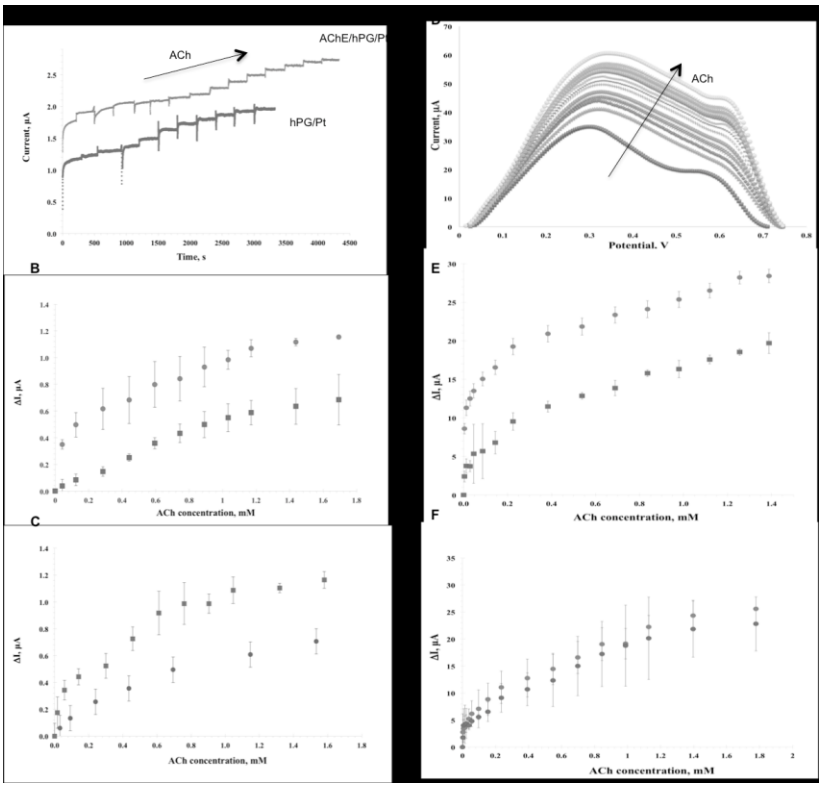

Figure 3 Chronoamperometry and SWV response of both the AChE/hPG/Pt and hPG/Pt electrodes for different concentrations of ACh, in either glycine or PBS buffer at pH 7.4 and in the presence of oxygen. • refers to AChE/hPG/Pt; ■ refers to hPG/Pt. Chronoamperometry at 0.3 V: A) an example of chronoamperometry readings in glycine; B) current change versus ACh concentration in the case of glycine buffer; C) current change versus ACh concentration at 0.3 V in the case of phosphate buffer. Square Wave Voltammetry: D) an example of SWV readings in glycine, AChE/hPG/Pt electrode only; E) change in the current peak at 0.3 V versus ACh concentration in the case of glycine buffer; F) change in the current peak at 0.3 V versus ACh concentration in the case of PBS. Error bars refer to three replicates.

Although the response to ACh and the shape of the calibration curves obtained with the two types of electrodes are very similar, the process occurring in each case is very different. In the case of AChE/hPG/Pt, choline is enzymatically generated (Step 1, Figure 1) and then oxidized by hPG (Step 2, Figure 1). In the other case, ACh is directly oxidized by hPG. To confirm this hypothesis, CV tests in the presence and absence of oxygen were performed (Figure 4). As shown, in the absence of oxygen AChE/hPG/Pt performs better, with a shift of approximately 0.06 mA. This is because Step 1 is favoured by the absence of oxygen. On the other hand, when hPG/Pt was operated in the absence of oxygen no response to ACh was observed, with a flat CV.

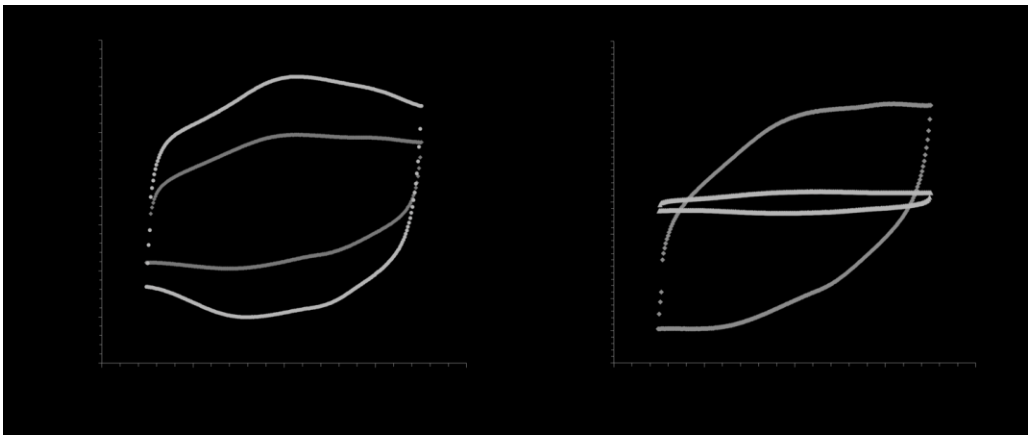

Figure 4- Cyclic voltammograms of both AChE/hPG/Pt (A) and hPG/Pt (B) electrodes in a PBS solution containing 0.6 mM of ACh in the presence (a) and absence (b) of oxygen. Scan rate: 50 mV s^{-1}

Considering the instability, cost and short lifetime of enzymes, a non-enzymatic sensor would be preferred. Nonetheless, enzymes are highly selective towards the target analyte. hPG is reactive to a number of compounds found in physiological fluids, such as sugars (du Toit and Di Lorenzo 2014a), and consequently a non-enzymatic hPG sensor would suffer from very poor selectivity. Practical applications of the hPG/Pt electrode would, therefore, necessarily imply the combined use of a functional membrane that filters out interfering compounds. This might prove difficult when these impurities have a molecular weight very close to ACh, such as glucose. We therefore focused on the enzymatic electrode only.

Table 1 summarizes the performance of AChE/hPG/Pt in both glycine and PBS resulting from the CA tests and Figure S1 A and B in the supplementary data show the relative calibration curves obtained. As reported, in the case of glycine buffer, the sensitivity was almost two times higher than the case of PBS, with a value of 3.04 $\mu A\ mM^{-1}\ cm^{-2}$, which corresponds to a slope of the calibration curve of approximately 0.5 $\mu A\ mM^{-1}$. This sensitivity is comparable to the values observed for other AChE electrodes found in previous works: 0.49 $\mu A\ mM^{-1}$ (Sen et al. 2004), and 0.42 $\mu A\ mM^{-1}$ (Doretti et al. 2000) and it is much higher than the sensitivity of a Cu-nanoparticle modified electrode with a sensitivity of only 0.23 $\mu A\ mM^{-1}\ cm^{-2}$ (Heli et al. 2009). On the other hand, a much higher sensitivity has been recently reported with a non enzymatic metal oxide nanostructure (Sattarahmady et al. 2013).

In the case of the non-enzymatic hPG/Pt electrode, the sensitivity is slightly higher, 4.6 $\mu A\ mM^{-1}\ cm^{-2}$, and also the linearity range is improved (Table 1S in the supplementary data).

From the reciprocal of the current - reciprocal of ACh concentration plot (Figure S3 and S4), it resulted a value of the apparent affinity, K_m^{app}, equal to 0.3 mM, which is in agreement with previous findings on AChE immobilised onto porous gold structures (Shulga et al. 2007). This is a value much lower than previously reported (Doretti et al. 2000; Sen et al. 2004), thus demonstrating the high affinity of AChE/hPG/Pt towards ACh.

Table 1. Analytical performance of the AChE/hPG/Pt electrode in both PBS and glycine buffer at pH 7.4.

	PBS	**Glycine**
Linearity range (mM)	0.24-1.9	0.12-1.4
Sensitivity ***($\mu A\ mM^{-1}\ cm^{-2}$)***	2.01 ± 0.7	3.40 ± 1.3
K_m^{app} ***(mM)***	0.30 ± 0.03	0.39 ± 0.2
R^2 (n=3)	0.98	0.98

R^2: correlation coefficient

3.2 Self-Powered detection of Acetylcholine in continuous flow mode

The AChE/hPG/Pt electrode was subsequently used as the anode of a flow-through membrane-less miniature fuel cell, with Pt as the cathode. The electrodes were connected through an external load and the system was continuously fed with PBS containing ACh at a flow rate of 0.35 ml min^{-1}. No external mediators were added to the feeding solution. Power and polarisation curves~~, performed~~ for increasing concentrations of ACh are shown in Figure 5. The polarisation curves exhibit a small activation region, a wide ohmic polarisation region and a short and steep mass transfer limitation region. This trend is in agreement with typical

polarisation curves obtained with biological fuel cells, where the ohmic losses play a dominant role (Logan et al. 2006). The polarisation curves up-shift with increasing concentrations of ACh and exhibit a corresponding open circuit potential within the range of 320 to 430 mV (Figure 5B). It is expected that AChE/hPG/Pt is the limiting electrode in the fuel cell. Considering the effect that oxygen has on the performance of this electrode, as shown in Figure 4A, the very low current densities obtained could also be due to the saturating concentration of oxygen in the feeding solution used in this study (0.2 mM). It should be noted, however, that physiological fluids, such as plasma, present much lower oxygen concentrations and could therefore be associated with improved performance of the fuel cell (Falk et al. 2012).

The power curves also show a good correlation between power output and ACh concentration (Figure 5A). The maximum power was of 4 nW at a voltage of 260 mV and for a current density of 9 μA cm^{-2} (ACh concentration: 10 mM). Since this is the first ACh/oxygen fuel cell reported, it is difficult to make a direct comparison on performance with other biological fuel cell devices reported in the literature, which are characterised by different device designs and catalyst used. Nonetheless, the performance of the ACh/O_2 hybrid fuel cell in terms of power output, is very similar to other biological fuel cells reported (Falk et al. 2013; Falk et al. 2012).

Although the power output is very low, the fuel cell showed an excellent response to varying acetylcholine concentrations, thus demonstrating its remarkable potential for use as a self-powered ACh sensor.

In Figure 5C a calibration curve is reported, obtained by connecting the two electrodes to an external resistor of 80 kΩ and varying the concentration of ACh in the feeding solution every 15 min. The response time, calculated as the time to reach 95% of the final, was in the range of 2.8-

3.7 min, being lower for higher ACh concentrations. This is a much faster response than other AChE-based sensors previously reported (Doretti et al. 2000; Schuvailo et al.).

The sensitivity of the sensor is of 0.1 μA mM^{-1} cm^{-2}, with a lower detection limit of 10 μM. This detection limit is in the range of ACh concentrations in healthy individuals, but still too high for patients affected by AD, characterised by ACh values of 1 – 6 μM (Chauhan and Pundir 2011). Still, these preliminary results are highly encouraging, and future research will necessarily have to focus on improving the fuel cell design and on maximising the electrode surface-area-to-volume ratio to enhance both the sensitivity and the limits of detection.

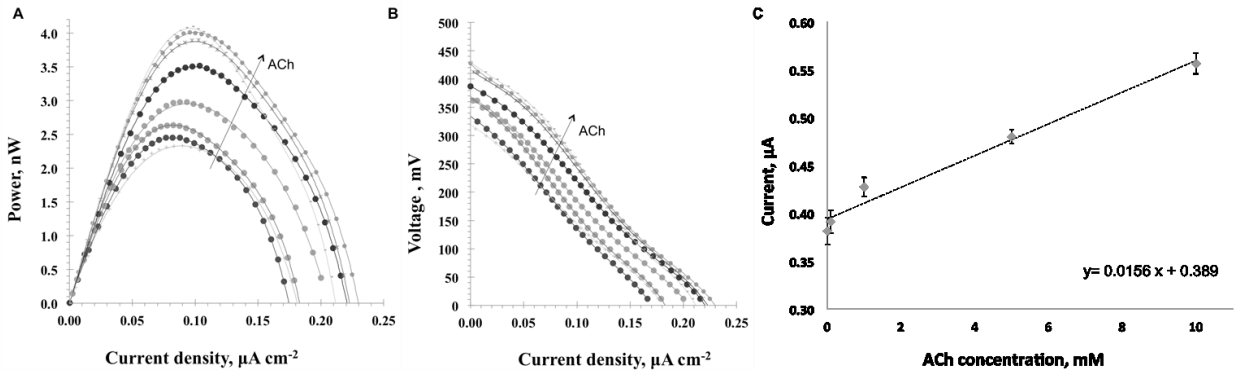

Figure 5. Power curves (A) and polarization curves (B) obtained with PBS solutions of ACh with a concentration varying from 0.01 to 10 mM in PBS. Current density refers to the geometric surface area of the anode (0.16 cm^2). (C) Current output generated by the flow-through AChE fuel cell at different ACh concentrations, for an external resistance of 80 kΩ. Error bars refer to at least two replicates.

The fuel cell sensor showed high reproducibility, as demonstrated by the very small variation among several replicates reported in Figure 5C. Although the lifetime of the device was not tested, the hybrid fuel cell here proposed is expected to be stable for at least two days of continuous operation, according to our previous findings with a glucose/oxygen EFC having a

similar set-up (du Toit and Di Lorenzo 2015). In addition, compared to this previous study where the laccase electrode was supposed to be the major limiting factor for the system stability, the use of a Pt cathode in the hybrid fuel cell might contribute to a substantial enhancement in the system lifetime (Ivanov et al. 2010). Finally, preliminary studies have demonstrated that the immobilization of AChE onto porous structures help to increase its overall stability (Shulga et al. 2007; Sotiropoulou et al. 2005).

CONCLUDING REMARKS

The development of rapid and low cost sensing devices for *in situ* monitoring of acetylcholine in plasma is key to enhance the therapy of the Alzheimer's disease. In patients affected by this serious neuro-degeneration, the levels of the neurotransmitter acetylcholine can drop by up to 90%. The consequence is a progressive and significant loss of cognitive and behavioural function. Effective *in vivo* monitoring of ACh can help with: timely diagnosis; monitoring treatment effectiveness; and developments of new medicines.

Current methodologies for ACh detection are mainly based on microdialysis coupled with offline analysis, and are expensive, slow and not suitable for *in situ* monitoring.

EFCs can provide an attractive alternative. In this study, we report the first acetylcholine/oxygen fuel cell and show an excellent response to ACh concentrations, in terms of both current and power output. No sample treatment is required and the response time is as fast as 3 min. As such, this research represents an important step towards self-powered low cost devices for the real time monitoring of ACh.

ACKNOWLEDGMENTS

Felismina T. C. Moreira acknowledges *Fundação para a Ciência e Tecnologia* for financial support (grant reference number: SFRH/BPD/97891/2013).

REFERENCES

http://ec.europa.eu/health/major_chronic_diseases/diseases/alzheimer/index_en.htm.

Barton, S.C., Gallaway, J., Atanassov, P., 2004. Enzymatic Biofuel Cells for Implantable and Microscale Devices. Chemical Reviews 104, 4867-4886.

~~Cai, J.R., Zhou, L.N., Han, E., 2014. A Sensitive Amperometric Acetylcholine Biosensor Based on Carbon Nanosphere and Acetylcholinesterase Modified Electrode for Detection of Pesticide Residues. Analytical Sciences 30(6), 669-673.~~

Cannon, M.J., Williams, A.D., Wetzel, R., Myszka, D.G., 2004. Kinetic analysis of beta-amyloid fibril elongation. Analytical Biochemistry 328(1), 67-75.

Castorena-Gonzalez, J.A., Foote, C., MacVittie, K., Halámek, J., Halámková, L., Martinez-Lemus, L.A., Katz, E., 2013. Biofuel Cell Operating in Vivo in Rat. Electroanalysis 25(7), 1579-1584.

Chauhan, N., Pundir, C., 2011. An amperometric biosensor based on acetylcholinesterase immobilized onto iron oxide nanoparticles/multi-walled carbon nanotubes modified gold electrode for measurement of organophosphorus insecticides. Analytica Chimica Acta 701, 66–74.

Davis, K., Berger, P., 1979. Brain Acetylcholine and Neuropsychiatric Disease. Plenum Press, New York.

Deng, L., Chen, C., Zhou, M., Guo, S., Wang, E., Dong, S., 2010. Integrated Self-Powered Microchip Biosensor for Endogenous Biological Cyanide. Analytical Chemistry 82(10), 4283-4287.

Doretti, L., Ferrara, D., Lora, S., Schiavon, F., Veronese, F.M., 2000. Acetylcholine biosensor involving entrapment of acetylcholinesterase and poly(ethylene glycol)-modified choline oxidase in a poly(vinyl alcohol) cryogel membrane. Enzyme and Microbial Technology 27, 279-285.

du Toit, H., Di Lorenzo, M., 2014a. Electrodeposited highly porous gold microelectrodes for the direct electrocatalytic oxidation of aqueous glucose. Sensors and Actuators B-Chemical 192, 725-729.

du Toit, H., Di Lorenzo, M., 2014b. Glucose oxidase directly immobilized onto highly porous gold electrodes for sensing and fuel cell applications. Electrochimica Acta 138, 86-92.

du Toit, H., Di Lorenzo, M., 2015. Continuous power generation from glucose with two different miniature flow-through enzymatic biofuel cells. Biosensors and Bioelectronics 69, 199-205.

du Toit, H., Rashidi, R., Ferdani, D.W., Delgado-Charro, M.B., Sangan, C.M., Di Lorenzo, M., 2016. Generating power from transdermal extracts using a multi-electrode miniature enzymatic fuel cell. Biosensors and Bioelectronics 78, 411–417.

Falk, M., Blum, Z., Shleev, S., 2012. Direct electron transfer based enzymatic fuel cells. Electrochimica Acta 82(1), 191-202.

Garguilo, M.G., Michael, A.C., 1995. Enzyme-modified electrodes for peroxide, choline, and acetylcholine Trends in Analytical Chemistry 14(4), 164-169

Garris, A, P., 2010. Advancing neurochemical monitoring. Nature methods 7(2), 106-108.

Halámková, L., Halámek, J., Bocharova, V., Szczupak, A., Alfonta, L., Katz, E., 2012. Implanted Biofuel Cell Operating in a Living Snail. Journal of the American Chemical Society 134(11), 5040-5043.

Hasselmo, M.E., Sarter, M., 2010. Modes and models of forebrain cholinergic neuromodulation of cognition. Neuropsychopharmacology 36, 52-73.

Heli, H., Hajjizadeh, M., Jabbari, A., Moosavi-Movahedi, A.A., 2009. Copper nanoparticles-modified carbon paste transducer as a biosensor for determination of acetylcholine. Biosenosrs and Bioelectronics 24(8), 2328–2333.

Hinman, C.L., Ernstoff, R.M., Montgomery, I.N., Hudson, R.A., Rauch, H.C., 1986. Clinical correlates of enzyme-immunoassay versus radioimmunoassay measurements of antibody against acetylcholine receptor in patients with myasthenia gravis. Journal of the Neurological Sciences 75(3), 305-316.

Hou, S., Ou, Z., Chen, Q., Wu, B., 2012. Amperometric acetylcholine biosensor based on self-assembly of gold nanoparticles and acetylcholinesterase on the sol-gel/multi-walled carbon nanotubes/choline oxidase composite-modified platinum electrode. Biosensors & Bioelectronics 33(1), 44-49.

Ivanov, I., Vidaković-Koch, T., Sundmacher, K., 2010. Recent Advances in Enzymatic Fuel Cells: Experiments and Modeling. Energies 3, 803-846.

Jia, W., Valdes-Ramírez, G., Bandodkar, A.J., Windmiller, J.R., Wang, J., 2013. Epidermal Biofuel Cells: Energy Harvesting from Human Perspiration. Angewandte Chemie international Edition 52, 7233 –7236

Kanai, M., Matsubara, E., Isoe, K., Urakami, K., Nakashima, K., Arai, H., Sasaki, H., Abe, K., Iwatsubo, T., Kosaka, T., Watanabe, M., Tomidokoro, Y., Shizuka, M., Mizushima, K., Nakamura, T., Igeta, Y., Ikeda, Y., Amari, M., Kawarabayashi, T., Ishiguro, K., Harigaya, Y., Wakabayashi, K., Okamoto, K., Hirai, S., Shoji, M., 1998. Longitudinal study of cerebrospinal fluid levels of tau, A beta 1-40, and A beta 1-42(43) in Alzheimer's disease: A study in Japan. Annals of Neurology 44(1), 17-26.

Kang, M., Lee, B., 2016. Sensing of bisphenol A and mercury ions in aqueous solutions using a functionalized porous gold electrode. Current Applied Physics 16, 446-452.

Kanik, F.E., Kolb, M., Timur, S., Bahadir, M., Toppare, L., 2013. An amperometric acetylcholine biosensor based on a conducting polymer. International Journal of Biological Macromolecules 59, 111–118.

Katz, E., Buckmann, A.F., Willner, I., 2001. Self-powered enzyme-based biosensors. Journal of the American Chemical Society 123(43), 10752-10753.

~~Kaur, B., Srivastava, R., 2015. A polyaniline-zeolite nanocomposite material based acetylcholinesterase biosensor for the sensitive detection of acetylcholine and organophosphates. New Journal of Chemistry 39, 6899-6906~~.

Kawanami, S., Tsuji, R., Oda, K., 1984. Enzyme-linked immunosorbent assay for antibody against the nicotinic acetylcholine receptor in human myasthenia gravis. Annals of Neurology 15(2), 195-200.

Leech, D., Kavanagh, P., Schuhmann, W., 2012. Enzymatic fuel cells: Recent progress. Electrochimica Acta 84, 223–234.

Li, S., Wang, Y., Ge, S., Yu, J., Yan, M., 2015. Self-powered competitive immunosensor driven by biofuel cell based on hollow-channel paper analytical devices. Biosensors & Bioelectronics 71, 18-24.

Logan, B.E., Hamelers, B., Rozendal, R., Schroeder, U., Keller, J., Freguia, F., Aelterman, P., Verstraete, W., Rabaey, K., 2006. Microbial Fuel Cells: Methodology and Technology. Environmental Science and Technology 40(17), 5181-5192.

MacVittie, K., Halamek, J., Halamkova, L., Southcott, M., Jemison, W.D., Lobel, R., Katz, E., 2013. From "cyborg" lobsters to a pacemaker powered by implantable biofuel cells. Energy & Environmental Science 6(1), 81-86.

Mayeux, R., Schupf, N., 2011. Blood-based biomarkers for Alzheimer's disease: plasma A beta 40 and A beta 42, and genetic variants. Neurobiology of Aging 32, S10-S19.

McKhann, G., Drachman, D., Folstein, M., Katzman, R., Price, D., Stadlan, E.M., 1984. Clinical diagnosis of Alzheimer's disease: Report of the NINCDS-ADRDA Work Group under the auspices of Department of Health and Human Services Task Force on Alzheimer's Disease. Neurology 34, 939-944.

Mitchell, K.M., 2004. Acetylcholine and choline amperometric enzyme sensors characterized in vitro and in vivo. Analytical Chemistry 76(4), 1098-1106.

Nguyen, Q.-T., Schroeder, L.F., Mank, M., Muller, A., Taylor, P., Griesbeck, O., Kleinfeld, D., 2010. An in vivo biosensor for neurotransmitter release and in situ receptor activity. Nature Neuroscience 13, 127–132.

Nirogi, R., Mudigonda, K., Kandikere, V., Ponnamaneni, R., 2010. Quantification of acetylcholine, an essential neurotransmitter, in brain microdialysis samples by liquid chromatography mass spectrometry. Biomedical Chromatography 24(1), 39-48.

Prince, M., Wimo, A., Guerchet, M., Ali, G.-C., Wu, Y.-T., Prina, M., 2015. World Alzheimer Report 2015. An anlysis of prevalence, incidence, cost and trends. Alzheimer's Disease International, London.

Reid, R., Minteer, S.D., Gale, B.K., 2015. Contact lens biofuel cell tested in a synthetic tear solution. Biosensors and Bioelectronics 68, 142–148.

Sattarahmady, N., Heli, H., Dehdari Vais, R., 2013. An electrochemical acetylcholine sensor based on lichen-like nickel oxide nanostructure. Biosensors and Bioelectronics 48, 197–202.

Sattarahmady, N., Heli, H., Dehdari Vais, R., 2014. A flower-like nickel oxide nanostructure: Synthesis and application for choline sensing. Talanta 119, 207–213.

Schuvailo, O.N., Dzyadevych, S.V., El'skaya, A.V., Gautier-Sauvigné, S., Csöregi, E., Cespuglio, R., Soldatkin, A.P., 2005Carbon fibre-based microbiosensors for in vivo measurements of acetylcholine and choline. Biosenosrs and Bioelectronics 21(1), 87-94.

Sekretaryova, A.N., Beni, V., Eriksson, M., Karyakin, A.A., Turner, A.P.F., Vagin, M.Y., 2014. Cholesterol Self-Powered Biosensor. Analytical Chemistry 86(19), 9540-9547.

Sen, S., Gulce, A., Gulce, H., 2004. Polyvinylferrocenium modified Pt electrode for the design of amperometric choline and acetylcholine enzyme electrodes. Biosensors and Bioelectronics 19(10), 1261–1268.

Shulga, O.V., Jefferson, K., Khan, A.R., D'Souza, V.T., Liu, J., Demchenko, A.V., Stine, K.J., 2007. Preparation and Characterization of Porous Gold and its Application as a Platform for Immobilization of Acetylcholine Esterase. Chemistry of Materials 19(16), 3902-3911.

Song, P., Hershey, N.D., Mabrouk, O.S., Slaney, T.R., Kennedy, R.T., 2012. Mass spectrometry "sensor" for in vivo acetylcholine monitoring. Analytical Chemistry 84(11), 4659-4664.

Sotiropoulou, S., Vamvakaki, V., Chaniotakis, N.A., 2005. Stabilization of enzymes in nanoporous materials for biosensor applications. Biosensors & Bioelectronics 20(8), 1674-1679.

Tandon, R., 1999. Cholinergic aspects of schizophrenia.

British Journal of Psychiatry 174, 7–11.

Uutela, P., Reinila, R., Piepponen, P., Ketola, R.A., Kostiainen, R., 2005. Analysis of acetylcholine and choline in microdialysis samples by liquid chromatography/tandem mass spectrometry. Rapid Communications in Mass Spectrometry 19(20), 2950-2956.

Van der Zee, E.A., Luiten, P.G., 1999. Muscarinic acetylcholine receptors in the hippocampus, neocortex and amygdala: a review of immunocytochemical localization in relation to learning and memory. Progress in Neurobiology 58(5), 409-471.

Wen, D., Deng, L., Guo, S., Dong, S., 2011. Self-Powered Sensor for Trace Hg2+ Detection. Analytical Chemistry 83(10), 3968-3972.

Wilson, G.S., Gifford, R., 2005. Biosensors for real-time in vivo measurements. Biosenosrs and Bioelectronics 15, 2388–2403.

Wise, D.D., Barkhimer, T.V., Brault, P.A., Kirchhoff, J.R., Messer, W.S., Hudson, R.A., 2002. Internal standard method for the measurement of choline and acetylcholine by capillary electrophoresis with electrochemical detection. Journal of Chromatography B-Analytical Technologies in the Biomedical and Life Sciences 775(1), 49-56.